

Identification of Amino Acids in the N-terminal Domain of Atypical Methanogenic-type Seryl-tRNA Synthetase Critical for tRNA Recognition^{*[5]}

Received for publication, July 22, 2009, and in revised form, August 25, 2009 Published, JBC Papers in Press, September 4, 2009, DOI 10.1074/jbc.M109.044099

Jelena Jaric[‡], Silvija Bilokapic[‡], Sonja Lesjak[‡], Ana Crnkovic[‡], Nenad Ban[§], and Ivana Weygand-Durasevic^{‡1}

From the [‡]Department of Chemistry, Faculty of Science, University of Zagreb, Horvatovac 102a, HR-10000 Zagreb, Croatia and the [§]Institute of Molecular Biology and Biophysics, Swiss Federal Institute of Technology, ETH Zurich, Zurich 8093, Switzerland

Seryl-tRNA synthetase (SerRS) from methanogenic archaeon *Methanosarcina barkeri*, contains an idiosyncratic N-terminal domain, composed of an antiparallel β -sheet capped by a helical bundle, connected to the catalytic core by a short linker peptide. It is very different from the coiled-coil tRNA binding domain in bacterial-type SerRS. Because the crystal structure of the methanogenic-type SerRS-tRNA complex has not been obtained, a docking model was produced, which indicated that highly conserved helices H2 and H3 of the N-terminal domain may be important for recognition of the extra arm of tRNA^{Ser}. Based on structural information and the docking model, we have mutated various positions within the N-terminal region and probed their involvement in tRNA binding and serylation. Total loss of activity and inability of the R76A variant to form the complex with cognate tRNA identifies Arg⁷⁶ located in helix H2 as a crucial tRNA-interacting residue. Alteration of Lys⁷⁹ positioned in helix H2 and Arg⁹⁴ in the loop between helix H2 and β -strand A4 have a pronounced effect on SerRS-tRNA^{Ser} complex formation and dissociation constants (K_D) determined by surface plasmon resonance. The replacement of residues Arg³⁸ (located in the loop between helix H1 and β -strand A2), Lys¹⁴¹ and Asn¹⁴² (from H3), and Arg¹⁴³ (between H3 and H4) moderately affect both the serylation activity and the K_D values. Furthermore, we have obtained a striking correlation between these results and *in vivo* effects of these mutations by quantifying the efficiency of suppression of bacterial amber mutations, after coexpression of the genes for *M. barkeri* suppressor tRNA^{Ser} and a set of mMbSerRS variants in *Escherichia coli*.

The aminoacyl-tRNA synthetases (aaRSs)² catalyze the activation of cognate amino acids and their transfer to the 3'-end of

corresponding tRNA molecules. The aaRSs are a highly conserved family of enzymes comprised of two distinct structural groups referred to as classes I and II (1–3), with a notable exception of LysRS representatives, which belong to both classes (4). Although the catalytic mechanisms of various aaRSs are broadly similar (5), each enzyme has developed a high specificity in recognizing its cognate amino acid and tRNA, which is pivotal for accurate translation of the genetic code (1). The discrimination of the amino acids is based on recognizing the differences in the size and charge of the molecules (6). The specificity of tRNA selection depends on a set of identity determinants that are mostly located at two distal extremities: the anticodon loop and the amino acid accepting stem. In a few instances, identity elements are also found in the D-arm, T-arm, and variable loop. They can either act as positive determinants that enhance aminoacylation or negative ones that prevent aminoacylation. The recognition of tRNAs by synthetases can also be affected by the modification of particular nucleotides (7, 8). AaRSs show divergent strategies for tRNA recognition. Most notably, class I and class II aaRSs (including pyrrolysyl-tRNA synthetase, see Ref. 9) approach tRNAs from the minor and major groove sides of the acceptor stem, respectively (10). Although the majority of determinants are in direct contact with cognate synthetases (8), the aminoacylation fidelity is controlled by kinetic differences more than by binding affinities (11).

Seryl-tRNA synthetases (SerRSs), which catalyze the aminoacylation of several tRNA^{Ser} isoacceptors and tRNA^{Sec} with serine, can be divided into two structurally different groups: bacterial-type SerRSs function in a variety of archaeal, bacterial, and eukaryotic organisms, whereas the methanogenic-type was found only in methanogenic archaea (12, 13). Furthermore, based on sequence comparison (14, 15) and x-ray analyses, two subgroups of bacterial-type SerRSs were identified: one consists of the enzymes from bacterial sources, best represented by those from *Thermus thermophilus* (16) and *Escherichia coli* (3), and an archaeal/eukaryal-type, structurally related to SerRS from archaeon *Pyrococcus horikoshii* (17).

All SerRSs are functional homodimers with a C-terminal active site domain typical for class II aaRSs and an N-terminal domain that is responsible for binding of the long variable arm of tRNA^{Ser} isoacceptors (reviewed in Ref. 18), with exception of the mammalian mitochondrial enzyme (19). The long variable arm of tRNA^{Ser} categorizes it as one of the type 2 tRNAs, including the tRNA^{Ser} and tRNA^{Leu} species (from all organisms

^{*} This work was supported by Ministry of Science, Education and Sports of the Republic of Croatia Project (119-0982913-1358), grants from the Swiss National Science Foundation, the Scientific Cooperation between Eastern Europe and Switzerland (SCOPEs) program of the Swiss National Science Foundation, and Unity through Knowledge Fund project 10/07.

^[5] The on-line version of this article (available at <http://www.jbc.org>) contains supplemental Table S1.

¹ To whom correspondence should be addressed. Tel.: 385-1-460-6230; Fax: 385-1-460-6401; E-mail: weygand@chem.pmf.hr.

² The abbreviations used are: aaRS, aminoacyl-tRNA synthetase (standard amino acid abbreviations precede RS throughout); SerRS, seryl-tRNA synthetase; mMbSerRS, methanogenic-type *Methanosarcina barkeri* SerRS; MbtRNA^{GGA}, *M. barkeri* tRNA^{Ser} with anticodon GGA; SPR, surface plasmon resonance; WT, wild type; DTT, dithiothreitol; Mes, 2-(*N*-morpholino)ethanesulfonic acid.

tRNA Binding Residues in mMbSerRS N-terminal Domain

or domains of life) and bacterial tRNA^{Tyr} species (20). In bacterial-type SerRS, the N-terminal domain forms an antiparallel α -helical coiled-coil structure (3, 16), whereas in the methanogenic-type counterpart it is significantly larger and composed of a six-stranded antiparallel β -sheet capped by a bundle of three helices (H1, H2, and H4) with up-down topology and an additional short helix (H3) that runs almost perpendicular to helix H4 (21) (see Fig. 1). Despite pronounced structural differences between the tRNA-binding domains in two SerRS types, in each case the N-terminal domain of one subunit interacts with the extra arm of tRNA^{Ser}, to position the 3'-end of tRNA into the C-terminal active site of another subunit (23–25). The recent crystal structure of the first archaeal/eukaryal SerRS from the archaeon *P. horikoshii*, and the structure-based model of the enzyme bound with the *T. thermophilus* and *P. horikoshii* tRNAs^{Ser}, suggested that the helical N-terminal domain of *P. horikoshii* SerRS is also involved in the binding of the extra arm of tRNA (17).

The recognition of tRNA by SerRS relies, besides on the long extra arm, on the identity elements in tRNA^{Ser} acceptor arms, achieved by the motif 2 residues. Unlike the majority of aaRSs systems, the anticodon triplet is not recognized by SerRS. The first four base pairs in the tRNA acceptor arm (G1:C72, G2:C71, A/U3:U/A70, and R4:Y69) are identity elements for bacterial SerRS, and among them, the second G2:C71 base pair is the most significant (reviewed in Ref. 18). Consistently, the crystal structure of the *T. thermophilus* SerRS•tRNA^{Ser} complex revealed that SerRS interacts with the tRNA^{Ser} acceptor stem, and Ser²⁶¹ is responsible for the base-specific interaction with G2 (23, 26). Although the acceptor stem sequences are not well conserved among the eukaryal tRNA^{Ser} isoacceptors, the discriminator base G73 is an essential identity requirement for human tRNA^{Ser} and serves as an anti-determinant in lower eukaryotes (reviewed in Ref. 18). Unlike eukaryal tRNAs^{Ser}, archaeal tRNAs^{Ser} conserve the G1:C72, C2:G71, C3:G70, and G4:C69 base pairs in the acceptor stem. However, the tRNA specificity of the archaeal/eukaryal SerRS from *P. horikoshii* seems to depend mainly on the extra arm, but not on the acceptor stem. Indeed, this enzyme exhibits quite relaxed specificity for tRNA^{Ser} recognition (17).

Archaeon *Methanosarcina barkeri*, which possesses two dissimilar SerRSs, one of a bacterial- and the other of methanogenic-type, provides an excellent system for studying the evolution of tRNA^{Ser} determinants. Two enzymes recognize the same set of tRNA isoacceptors *in vitro* (27). We have undertaken several approaches to elucidate the basis for their different serylation mechanisms. Kinetic analysis of variant tRNA^{Ser} transcripts by the two archaeal SerRS enzymes (27) revealed that the length of the variable arm is a critical recognition element for both enzymes, as is the identity of the discriminator base (G73) and base pair G30:C40 in the anticodon stem. However, additional determinants were identified as being required for specific serylation by the unusual methanogenic-type enzyme, which relies on G1:C72 identity and on the number of unpaired nucleotides at the base of the variable loop. The tRNA recognition pattern by two *M. barkeri* SerRS may differ *in vivo*, because only bacterial-type SerRS complements the function of thermolabile *E. coli* SerRS (28).

EXPERIMENTAL PROCEDURES

Site-directed Mutagenesis and Purification of Proteins—The seryl-tRNA synthetase expression vector (pET15bmMbSerRS) has been reported previously (27). Primers listed in [supplemental Table S1](#) and the QuikChange mutagenesis kit (Stratagene) were used for site-directed mutagenesis. Point mutations were confirmed by DNA sequencing.

Wild type and mutated SerRS proteins were expressed in *E. coli*, as described previously (21). Because WT mMbSerRS and its variants are His-tagged, they were first purified by affinity chromatography on nickel-nitrilotriacetic acid-agarose. Greater purity of proteins was achieved using cation exchange chromatography. Proteins were loaded on a Resource S 6-ml column and eluted with a linear KCl gradient (100–500 mM) in buffer containing 25 mM Mes, pH 6.2, 5 mM dithiothreitol (DTT), and 10 mM MgCl₂. Fractions enriched in SerRS were pooled and desalted on gel-filtration columns (PD-10), concentrated by ultrafiltration, and stored at –80 °C in a buffer containing 25 mM Hepes, pH 7.0, 200 mM KCl, 5 mM MgCl₂, 5 mM DTT, and 10% glycerol.

tRNA Cloning and *In Vitro* Transcription—The gene for MbtRNA^{Ser}_{GGA} was constructed from synthetic oligomers according to the published sequence (27). *In vitro* transcription was performed as reported previously (29). The tRNA transcript was carefully renatured prior to use in the kinetic assay, gel mobility shift assay, and surface plasmon resonance spectroscopy by heating for 5 min at 70 °C in 10 mM Tris/HCl, pH 7.5, followed by addition of MgCl₂ to the final concentration of 5 mM and placing on ice. MbtRNA^{Ser}_{GGA} was maximally serylated to 80% as determined in the standard reaction mixture (described below).

Aminoacylation Assay—Aminoacylation was carried out at 37 °C in the reaction mixture containing 50 mM Hepes/HCl, pH 7.0, 15 mM MgCl₂, 4 mM DTT, 5 mM ATP, 125 μ M [¹⁴C]serine, 0.25 μ M SerRS, and 1.5 μ M tRNA. Quantification of synthesized radioactive seryl-tRNA^{Ser} was done as described (29). Relative serylation rates represent the average of at least three independent experiments.

Electrophoretic Mobility Shift Assay—To check for complex formation between cognate tRNA and wild type or mutated mMbSerRS a constant amount of purified protein (8.3 pmol) was mixed with tRNA (14.8 pmol) and incubated for 15 min at 37 °C in a 13.5- μ l volume containing 30 mM Hepes, pH 7.0, and 6 mM MgCl₂ followed by cooling on ice. To test salt influence on non-covalent complex formation between protein and nucleic acid, salt (25 or 250 mM KCl) at different amounts was added in the reaction mixture prior to incubation for 15 min at 37 °C. Samples were subjected to electrophoresis on a native 9% acrylamide (w/v) gel of acrylamide:bis-acrylamide (19:1) containing 5% glycerol in electrophoresis buffer (25 mM Mes, 25 mM Tris, pH 7.6). Electrophoresis was performed at 4 °C for 2.5 h at 120 V, and gels were stained with silver.

Surface Plasmon Resonance—Kinetic studies were performed at 25 °C using a BIACORE T100 surface plasmon resonance (SPR) instrument. Wild type protein and mutants were covalently attached to a carboxymethyl dextran-coated gold surface (CM5 sensor chip). The carboxymethyl groups of dex-

tRNA Binding Residues in mMbSerRS N-terminal Domain

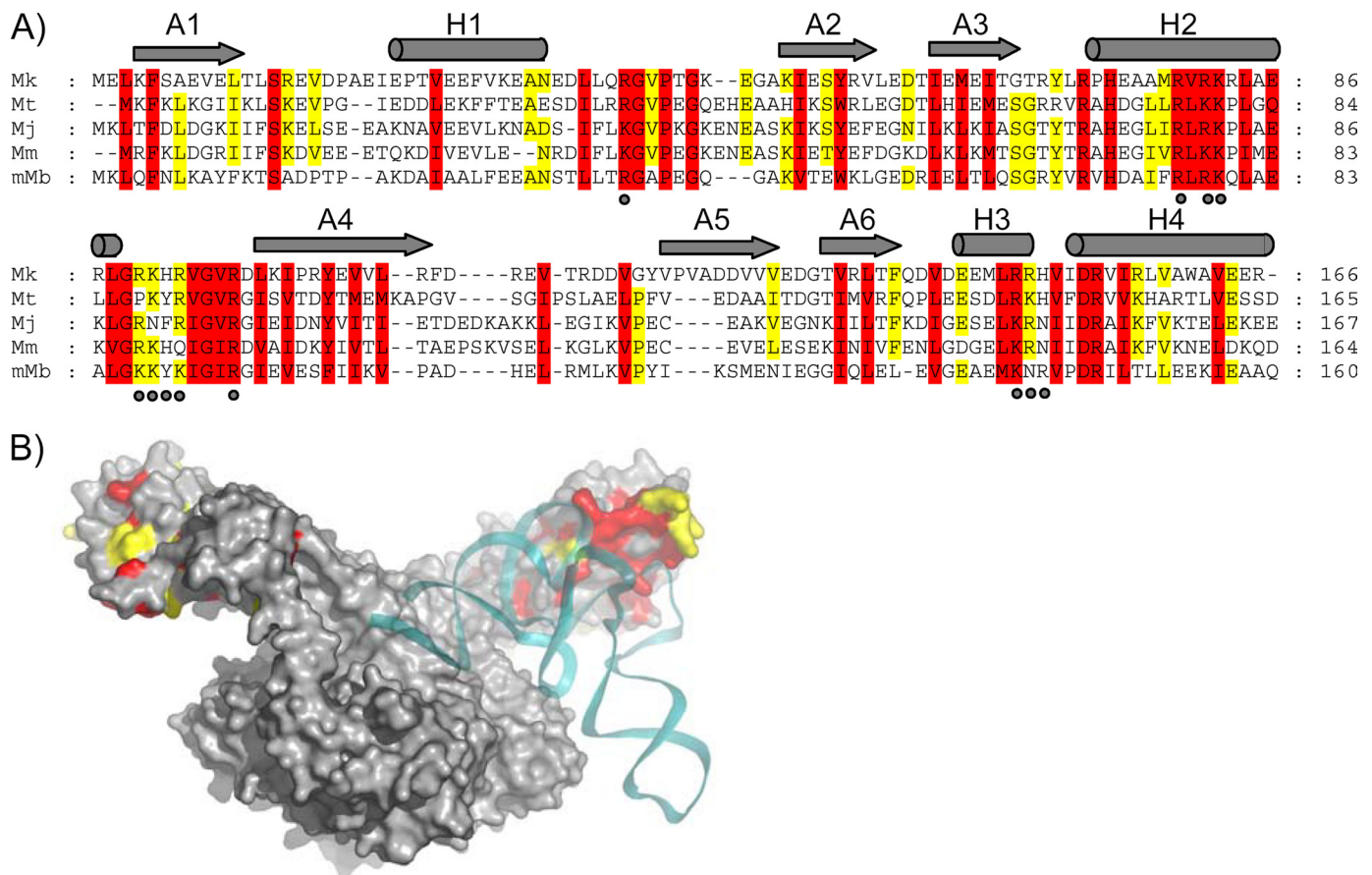


FIGURE 1. Design of mMbSerRS variants based on the conserved amino acid residues in the N-terminal domain of methanogenic-type SerRSs and their proximity to tRNA in mMbSerRS-tRNA^{Ser} docking model. *A*, the structure-based sequence alignment of the mMbSerRS N-terminal domain with selected SerRS sequences derived from methanogenic archaea (*Mk*, *Methanopyrus kandleri*; *Mt*, *Methanothermobacter thermoautotrophicus*; *Mj*, *Methanococcus jannaschii*; *Mm*, *Methanococcus maripaludis*; *mMb*, *Methanosarcina barkeri*). The sequence alignment was generated using the program MUSCLE (22). Amino acids that are completely conserved are in red, whereas those with 80% conservation are in yellow. Secondary structural elements are indicated above the alignment with gray cylinders and arrows for helices and β -sheets, respectively. Mutated residues are marked with dots. *B*, mMbSerRS-tRNA^{Ser} docking model. The SerRS dimer is shown in gray and tRNA^{Ser} is colored cyan. Conserved amino acids are indicated by the same color code as in *A*.

tran were activated with 1-ethyl-3-(3-dimethylaminopropyl)-carbodiimide hydrochloride and *N*-hydroxysuccinimide, and seryl-tRNA synthetase, or its mutants, were attached at pH 5.0 in 10 mM sodium acetate. Any remaining reactive sites were blocked by reaction with ethanolamine and the surface was washed with 50 mM NaOH to remove any non-covalently bound ligand. Proteins were immobilized at levels of 1000 response units in one flow cell. The kinetics of association and dissociation were monitored at a flow rate of 60 μ l/min. The renatured tRNA analyte was diluted in a running buffer (30 mM Hepes, pH 7.0, 6 mM MgCl₂, and 5 mM DTT). Binding was measured at concentration ranges of 19.5 nM to 8 μ M tRNA. After the end of each injection, tRNA was allowed to dissociate for 500 s and then the chip was regenerated with 3 M KCl at a flow of 100 μ l/min for 5 min. Data reported are the differences in SPR signal between the flow cell containing the wild type or mutant mMbSerRS and the reference cell without enzyme immobilized. Duplicate injections were made for each tRNA concentration in one round of measurement and each experiment was repeated twice. The data were analyzed using Biacore T100 Evaluation Software.

Suppression of *E. coli* Amber Mutations—The assay is based on monitoring the suppression efficiency of bacterial amber

mutations in *E. coli* strain XAC-A24 (*F'* *ara argE(UAG) rpoB gyrA Δ lac pro/F'* *lacI(UAG)-Z proAB*) (28), after co-expression of the *M. barkeri* SerRS gene, encoding methanogenic-type SerRS, with the gene for cognate archaeal suppressor tRNA (supMb). The synthetic gene for supMb, bearing the CGA anticodon, was inserted into the pTech plasmid, behind the *lpp* promoter, as described (28). To obtain higher expression of genes of some SerRS mutants, NcoI–XhoI fragments containing synthetase genes with the N-terminal His₆ tag from plasmid pET15b were then recloned into pBAD24 vector (30), where SerRS expression is under control of the arabinose inducible promoter. Suppression of the *argE* amber mutation was tested by plating *E. coli* cells on selective M9 minimal glucose plates. The efficiency of suppression was determined by measuring the β -galactosidase activity produced from *lacI-lacZ* fusion harboring a nonsense mutation in the *lacI* portion (31).

RESULTS

Selection of Target Sites for Site-directed Mutagenesis—Our previously published structure-based model of the mMbSerRS-tRNA^{Ser} complex (Fig. 1) implies that tRNA^{Ser} binds across two subunits of dimeric enzyme, as observed in the bacterial synthetase-tRNA complex structure. Experimental verification

tRNA Binding Residues in mMbSerRS N-terminal Domain

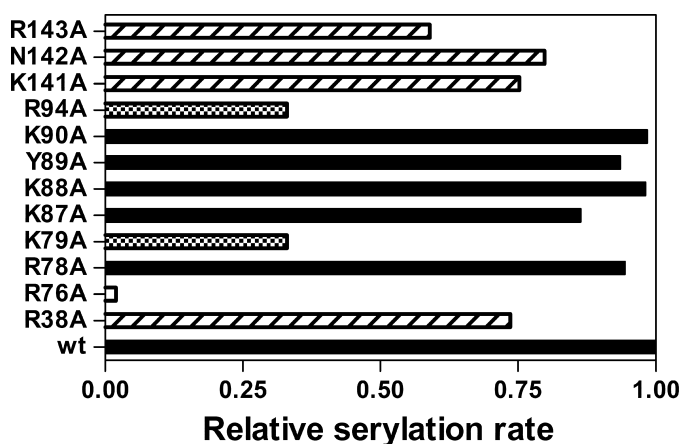


FIGURE 2. Aminoacylation activity of mMbSerRS variants. Relative serylation rates of *in vitro* transcribed MbtRNA^{Ser} by mMbSerRS variants are presented by horizontal bars. Mutated enzymes that retain the serylation ability comparable with the WT enzyme are colored black, mutants with the serylation rate lowered to 59–80% of the WT are designated with traverse lines, variants with a significant drop in the serylation rate (33% of the WT serylation rate) are marked with a black and white square pattern, and one which completely loses the serylation ability is highlighted white.

of predicted cross-dimer binding was provided by testing the activity of constructed SerRS heterodimers (25). In the model the long variable arm of the tRNA is positioned to interact with the N-terminal domain of mMbSerRS, in accordance with our previous biochemical experiments that identified the long variable arm of archaeal tRNA^{Ser} as a major tRNA recognition determinant (27, 29, 32). Furthermore, electrostatic potential calculations of the mMbSerRS dimer show an extended area of positive surface potential on the inner bow of the N-terminal domain, supporting the idea of N-terminal domain involvement in recognition of the negatively charged tRNA backbone (21). As target sites for mutagenesis we have chosen positions encoding highly conserved amino acids in the N-terminal domain of mMbSerRS (marked by dots in Fig. 1A), that are according to the docking model, in the proximity of tRNA (Fig. 1B). In all constructed mMbSerRS variants (listed in [supplemental Table S1](#)) a single amino acid was replaced with alanine: arginine 38, arginine 76, arginine 78, lysine 79, lysine 87, lysine 88, tyrosine 89, lysine 90, arginine 94, lysine 141, asparagine 142, and arginine 143. Most altered residues carry basic side chains expected to interact with negatively charged tRNA. Functional characterization of mMbSerRS mutants was performed *in vitro* and *in vivo*.

A Single Amino Acid Change (R76A) Causes Complete Loss of Aminoacylation Activity—Serylation propensity of all SerRS variants was tested in a standard aminoacylation assay with *in vitro* transcribed MbtRNA^{Ser}_{GGA} as a substrate (Fig. 2). Mutant R76A completely failed to serylate tRNA^{Ser}, a notable drop in aminoacylation activity was detected for mutants K79A and R94A, whereas mMbSerRS variants carrying R38A, K141A, N142A, and R143A replacements revealed moderately decreased initial serylation rates in comparison with WT MbSerRS. Structural integrity of the variant carrying the R76A replacement was probed by circular dichroism, which confirmed that the observed lack of tRNA charging capacity was not caused by protein misfolding (data not shown). This is also supported by the ability of the R76A, K79A, R94A, and R143A

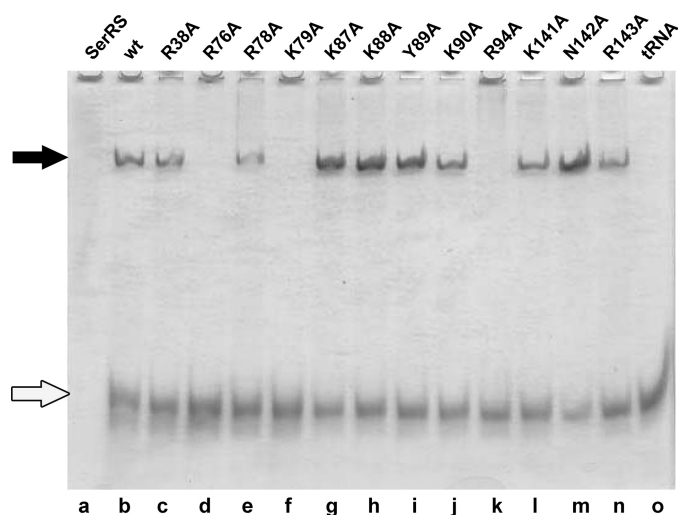


FIGURE 3. Gel mobility shift assay of the non-covalent complexes between MbtRNA^{Ser} and various mMbSerRS mutants. MbtRNA^{Ser} was incubated with different mMbSerRS variants (final concentration of tRNA and enzymes was 1.1 and 0.6 μ M, respectively) and subjected to PAGE under native conditions: WT, lane b; R38A, lane c; R76A, lane d; R78A, lane e; K79A, lane f; K87A, lane g; K88A, lane h; Y89A, lane i; K90A, lane j; R94A, lane k; K141A, lane l; N142A, lane m; and R143A, lane n. Non-complexed mMbSerRS (8.3 pmol) and MbtRNA^{Ser} (14.8 pmol) were loaded on the gel as electrophoretic mobility markers (lanes a and o, respectively). Non-covalent complexes and non-complexed tRNA are marked with black and white arrows, respectively.

mutants to catalyze amino acid activation in the pyrophosphate exchange reaction (data not shown).

Gel Retardation Assay Reveals Amino Acids Crucial for Non-covalent Complex Formation with Cognate tRNA—All mMbSerRS variants were tested for the ability to participate in the non-covalent complex formation with *in vitro* transcribed MbtRNA^{Ser}_{GGA} (Fig. 3). Mutants R38A, R78A, K87A, K88A, Y89A, K90A, K141A, N142A, and R143A formed complexes stable enough to be detected on the gel (Fig. 3, lanes c, e, g–j, and l–n, respectively), whereas the variant R76A did not form a complex, as expected. Because the interactions between synthetase and tRNA are in general electrostatic, raising the salt concentration may affect the stability of the complexes. Gel mobility shift assay was thus performed in the presence of 25 and 250 mM KCl (Fig. 4) for the wild type enzyme and mutants with moderately decreased serylation propensity (R38A, K141A, and R143A). As shown in Fig. 4A the complexes involving mutants R38A and R143A are much weaker in the presence of 10-fold higher salt (lanes g and i, respectively, in comparison with lanes c and e), whereas the K141A-tRNA complex vanishes completely (lane h in comparison with lane d). Thus, amino acids Arg³⁸, Lys¹⁴¹, and Arg¹⁴³ seem to be involved in non-covalent complex formation. Moreover, diminished serylation activities of these mutants in the presence of a higher salt concentration emphasize their involvement in ionic interactions (Fig. 4B). The activity of the WT enzyme at 25 mM KCl was used as the reference point (100% activity) and the activities of WT SerRS, R38A and K141A enzymes were determined at salt concentrations of 125 and 250 mM. Evidently, the activity of mutants drops more rapidly than the enzyme activity of the WT. More precisely, there is a 60% drop in activity of mutated enzymes when the concentration of KCl was increased from 25 to 125 mM, whereas in the case of the wild type enzyme activity

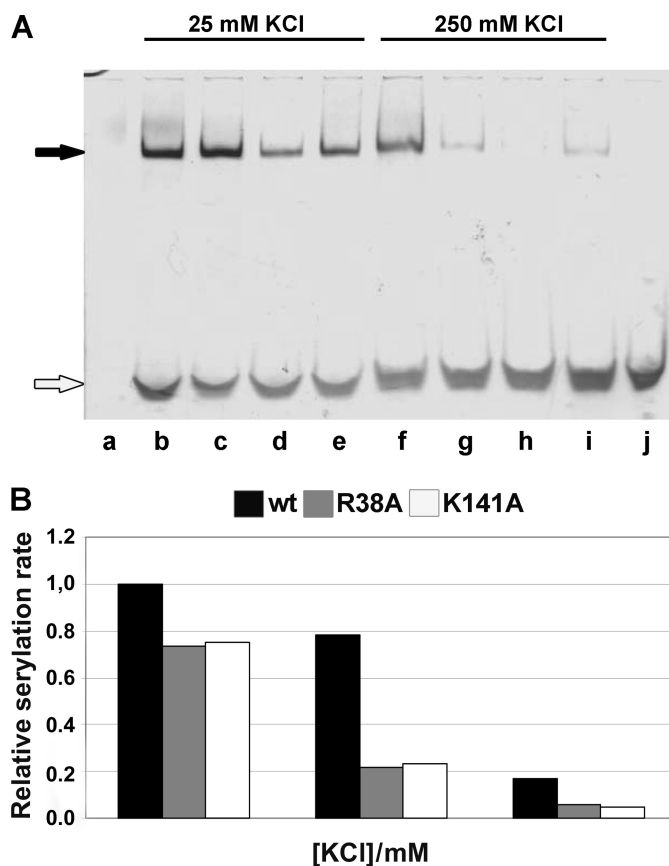


FIGURE 4. Effect of different salt concentrations on non-covalent complex formation and serylation propensity. *A*, non-covalent complexes were made as described under “Experimental Procedures” and in the legend to Fig. 3, except that in the reaction mixture the concentration of KCl was varied as indicated, and then subjected to PAGE under native conditions. Non-complexed WT mMbSerRS is visible in lane *a*, whereas non-covalent complexes between tRNA and mMbSerRS variants in the presence of 25 mM KCl were loaded into following lanes: WT, lane *b*; R38A, lane *c*; K141A, lane *d*; and R143A, lane *e*; non-covalent complexes between tRNA and mMbSerRS variants in the presence of 250 mM KCl were loaded into following lanes: WT, lane *f*; R38A, lane *g*; K141A, lane *h*; and R143A, lane *i*; non-complexed tRNA is in lane *j*. Non-covalent complexes and non-complexed tRNA are marked with black and white arrows, respectively. *B*, relative serylation rate of the enzymes was tested at three different KCl concentrations (25, 125, and 250 mM). Activity of the WT enzyme at 25 mM KCl was taken as the reference point (100% activity). Contrary to the WT enzyme, a significant drop in the serylation rate was detected for both mutants after raising the KCl concentration from 25 to 125 mM.

drops only 20% (and the enzyme is still around 80% active in the presence of 125 mM KCl). Although inactive in tRNA complex formation, the capacity of mutants K79A and R94A to catalyze the formation of seryl-adenylate remained comparable with the wild type enzyme, as revealed by a PP_i -exchange assay (not shown).

Determination of Dissociation Constants for tRNA·mMbSerRS Complexes by SPR Reveals the Importance of Arg⁹⁴ in tRNA Binding—We used SPR to compare the interaction of 12 mMbSerRS proteins (WT enzyme and 11 mutants) and tRNA. The study was performed on a CM5 sensor chip on which the WT SerRS and the variants were independently immobilized. Different concentrations of tRNA were injected at a flow rate of 60 μ l/min for 210 s. The sensorgram obtained for the WT enzyme agreed best with a two-state binding model with a conformational change, described by the following equation,

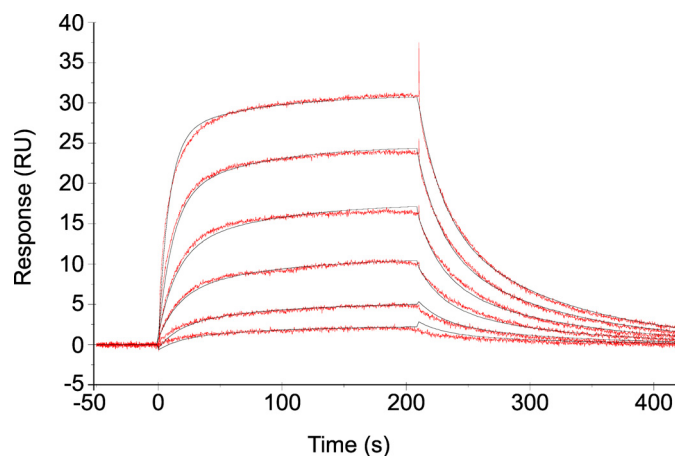
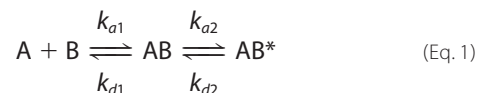


FIGURE 5. Kinetic analysis of tRNA binding to immobilized mMbSerRS R143A monitored by a biosensor. Sensorgrams (red) were obtained for the binding of different concentrations of tRNA^{Ser} (70.3–2250 nM) in 30 mM Hepes, pH 7.0, 6 mM MgCl₂, and 5 mM DTT to R143A mMbSerRS. Data were fit to the two-state conformational change model (black).



where $K_A = (k_{a1}/k_{d1})(1 + k_{a2}/k_{d2})$ and $K_D = 1/K_A$. In this model, the analyte A (tRNA) binds to the ligand B (mMbSerRS) to form an initial complex AB. The complex then undergoes a change in conformation to form a more stable complex AB* (33). The sensorgrams of all other mutants agreed best with the two-state binding model with conformational change as well, except for mutant R94A. Curves obtained for this mutant could have been interpreted only by using the steady state affinity model. In that sense, the K_D value (without k_{a1} , k_{d1} , k_{a2} , and k_{d2} constants) was solely determined for the R94A variant. An example of the sensorgram, denoting tRNA binding to the R143A variant, and the kinetic constants calculated from the fitted curves, are given in Fig. 5 and Table 1, respectively. SPR analysis for mutant R76A was not performed because that particular enzyme was inactive in aminoacylation and did not form a non-covalent complex detectable on the gel. According to the data presented in Table 1 the largest effect on binding the tRNA was achieved by altering arginine 94 to alanine. The K_D value for the R94A mutant was almost 50-fold higher than for the wild type enzyme (122 nM for the WT enzyme and 5.81 μ M for the R94A variant). A significant effect on interaction with tRNA have mutations of lysines 79 and 141 and arginine 143. Their respective mutants K79A, K141A, and R143A have between 4- and 7-fold higher K_D values than the wild type enzyme. Variants R38A and N142A gave similar K_D values (422 nM and 386 nM, respectively) that were \sim 3.5-fold higher than the wild type K_D . Dissociation constants for all other mutants (R78A, K87A, K88A, Y89A, and K90A) ranged from 151 to 301 nM.

The first association constant, k_{a1} (constant of initial complex formation), is in the range of $10^4 \text{ M}^{-1} \text{ s}^{-1}$ for most of the mutants. Only the wild type enzyme and variants K88A and N142A have $1.175 \times 10^5 \text{ M}^{-1} \text{ s}^{-1} \leq k_{a1} \leq 1.471 \times 10^5 \text{ M}^{-1} \text{ s}^{-1}$ (Table 1), which is a value between 2- and 6-fold higher k_{a1} than for other mutated mMbSerRSs. The first-order rate constants (k_{a2}) for WT, R78A, K87A, K88A, Y89A, and K90A were 2–6-

TABLE 1

Kinetic constants obtained from the fit to the conformational change model of sensorgrams acquired for the binding of different concentrations of tRNA (19.5 nM to 8 μM) to various SerRS mutants

Only for mutant R94A steady state affinity model was used (see text).

SerRS variant	k_{a1}	k_{d1}	k_{a2}	k_{d2}	K_D	Relative K_D^a	χ^{2b}
	$M^{-1}s^{-1}/10^5$	$s^{-1}/10^{-1}$	$s^{-1}/10^{-2}$	$s^{-1}/10^{-3}$	$M/10^{-7}$		
WT	1.471 ± 0.010	1.239 ± 0.009	1.482 ± 0.006	2.513 ± 0.003	1.22	1	2.71
R38A	0.442 ± 0.001	0.342 ± 0.001	0.832 ± 0.004	9.949 ± 0.017	4.22	3.5	0.20
R78A	0.558 ± 0.002	0.417 ± 0.002	1.204 ± 0.004	4.192 ± 0.006	1.93	1.6	0.28
K79A	0.299 ± 0.001	0.231 ± 0.001	0.283 ± 0.002	7.543 ± 0.029	5.61	4.6	0.18
K87A	0.983 ± 0.013	0.714 ± 0.011	1.345 ± 0.014	3.552 ± 0.011	1.52	1.2	1.95
K88A	1.175 ± 0.004	0.862 ± 0.003	0.993 ± 0.002	2.703 ± 0.002	1.57	1.3	0.53
Y89A	0.568 ± 0.002	0.498 ± 0.003	1.048 ± 0.004	5.494 ± 0.008	3.01	2.5	0.20
K90A	0.572 ± 0.005	0.547 ± 0.006	1.606 ± 0.005	4.568 ± 0.006	2.12	1.7	0.77
R94A					58.10 ± 1.70	47.6	0.07
K141A	0.264 ± 0.001	0.237 ± 0.001	0.515 ± 0.003	6.169 ± 0.013	4.89	4.0	1.34
N142A	1.423 ± 0.005	1.212 ± 0.004	0.673 ± 0.002	5.578 ± 0.005	3.86	3.2	0.77
R143A	0.324 ± 0.001	0.444 ± 0.002	0.605 ± 0.004	11.27 ± 0.03	8.90	7.3	0.09

^a Relative K_D is determined as $K_D(\text{mutant})/K_D(\text{WT})$.^b Statistical value describing the closeness of fit. Values <10 are acceptable (34).

fold larger than k_{d2} ; these mutants have K_D values similar to the dissociation constant of the wild type (1.2–2.5 K_D of the wild type enzyme). In the case of the N142A, k_{a2} is just slightly higher than k_{d2} , whereas mutants R38A, K79A, K141A, and R143A have second dissociation rate constants (k_{d2}) even greater than k_{a2} . Their K_D values are at least 3.5-fold larger than K_D for the WT enzyme. The SPR experiment also allowed the estimation of so called " K_{D1} " (K_D of the first reaction of the two-step mechanism; $K_{D1} = k_{d1}/k_{a1}$), which is similar for all the mutants. Taken together, our results suggest that the second step of the reaction predominantly determines the observed K_D values.

Effects of Engineered mMbSerRS Amino Acid Alterations on Serylation of tRNA *In Vivo*—We have recently shown that expression of the gene encoding *M. barkeri* bacterial-type SerRS (bMbSerRS) in *E. coli* complements the function of thermolabile SerRS at the nonpermissive temperature, whereas expression of the mMbSerRS gene does not (28). However, co-expression of the *M. barkeri* seryl-tRNA synthetase gene, encoding either bacterial- or methanogenic-type SerRS, with the gene for the cognate archaeal suppressor tRNA leads to suppression of bacterial amber mutations, implying that the *E. coli* translation machinery can use serylated tRNA from methanogenic archaea as a substrate in protein synthesis (28). Bacterial strain XAC-A24 carries two amber mutations XAC-A24 (*E'* *ara argE(UAG) rpoB gyrA Δlac pro/F' lacI(UAG)-Z proAB*), suppression of which reflects recognition and aminoacylation levels of suppressor tRNA by selected aminoacyl-tRNA synthetases. The *argE(UAG)* mutation is suppressible by any amino acid. The other suppressible marker in strain XAC-A24, in which the UAG in-frame codon has been inserted in the *lacI* part of a *lacI-lacZ* fusion gene, was used for quantification of suppression efficiency (35, 36). Because serylation of *M. barkeri* serine-specific tRNA by endogenous *E. coli* SerRS is negligible (12, 37), suppression is entirely dependent on recognition between archaeal partners (mMbSerRS/suppressor tRNA^{Ser}). Serine-specific tRNAs are especially suitable to be used in such assays, because the anticodon is not a recognition element for interaction with the cognate synthetase, and its alteration does not change the tRNA identity (38). We have converted the tRNA_{CGA}^{Ser} isoacceptor sequence into the tRNA^{Ser} suppressor sequence (*supSMb*) and placed it behind the *lpp*

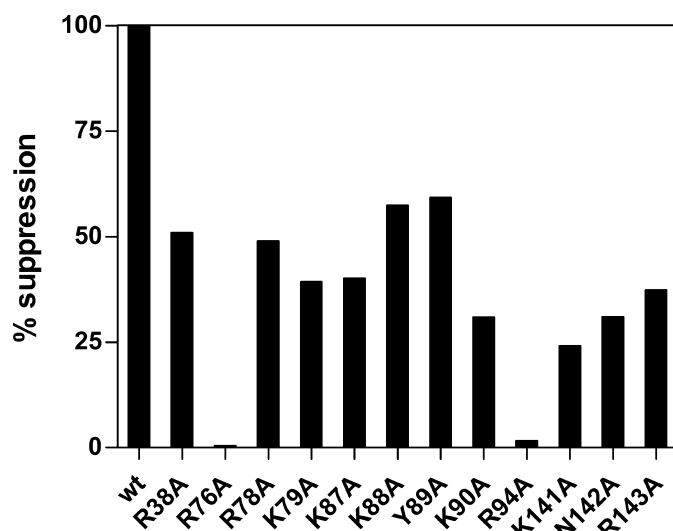


FIGURE 6. **Suppression efficiency of *M. barkeri* SerRS variants.** Suppression efficiency was determined by measuring the β -galactosidase activity in *E. coli* strain XAC-A24. 100% corresponds to the β -galactosidase activity of strain XAC-A24 co-transformed with the pET15b plasmid, carrying the gene for a wild type mMbSerRS, and pTech vector, carrying the *M. barkeri* suppressor tRNA^{Ser} sequence. Results were reported as the percentage of mutant enzyme suppression activity relative to that of the wild type enzyme.

promoter in the pTech plasmid (pTech^{supSMb}, see Ref. 28). Next, strain XAC-A24 was co-transformed with a pair of compatible plasmids, one of which carried the gene for a methanogenic-type synthetase variant, whereas the second carried the *M. barkeri* suppressor tRNA^{Ser} sequence. To analyze the contribution of individual amino acids to tRNA binding and catalysis, enzyme variants were characterized by the ability to serylate the suppressor tRNA *in vivo*. Expression of WT synthetase or its mutated variants was either from the pET15b plasmid, which enables constitutive expression by inefficient recognition of T7 promoter by bacterial RNA polymerase (28), or from pBAD24, where it is dependent on induction with arabinose (30). Expression of all mMbSerRS variants in the XAC-A24 strain has been verified by Western blot. No suppression was obtained when mMbSerRS variants, R76A and R94A, were co-expressed with archaeal suppressor tRNA (0 and 1.65% activity, respectively; Fig. 6). To exclude the possibility that the lack of

suppression was caused by too low expression of two synthetase variants from the pET15b plasmid, their genes were recloned to pBAD24 vector. Higher expression of the mutated synthetase R94A led to production of slightly higher quantities of serylated suppressor tRNA (from 1.65 to 7% suppression efficiency relative to the WT enzyme). This increment of the suppression level shows that in the case of the R94A mutant a weak suppression is possible. Alteration of residue Arg⁷⁶ resulted in an enzyme that was completely inactive *in vivo* (0% activity) regardless of which plasmid, pET15b or pBAD24, was used (see Fig. 6). These results are fully in agreement with our *in vitro* experiments performed with both mutants. Mutants K79A, K90A, K141A, N142A, and R143A displayed reduced suppression efficiency (Fig. 6) compared with the wild type mMbSerRS, confirming the contribution of these side chains in the interactions with tRNA. All other tested variants (R38A, R78A, K87A, K88A, and Y89A) showed more than 40% of the original suppression efficiency detected by the WT enzyme.

DISCUSSION

Idiosyncratic N-terminal Domains of SerRS Enzymes Provide tRNA^{Ser} Binding Capacity—The canonical tRNA^{Ser} is characterized by a long variable arm (B20 bases) between the anticodon stem and the T-arm, which SerRS employs as a major tRNA identity element to discriminate its cognate tRNAs from all other species. This elongated variable arm is well conserved throughout the evolutionary process from prokaryotes to eukaryotes (with the only exception being metazoan mitochondria). Accordingly, SerRS enzymes have acquired a unique N-terminal domain, mostly structured as a coiled-coil (3, 16, 17), for recognizing the variable arm. The N-terminal coiled-coil of *P. horikoshii* SerRS (17) comprises additional basic residues as compared with bacterial SerRSs (3, 16) and a Trp residue (Trp⁴⁰) found in other archaeal/eukaryal serine-specific synthetases (17). An insertion of 20 amino acids into the N-terminal sequences of metazoans and trypanosomatid SerRS sequences, at the center of the predicted coiled-coil motif, suggests that this region may extend beyond the length seen in the structures solved so far (39). On the other hand, although the coiled-coiled N-terminal domain exists in the metazoan mitochondrial SerRS, it does not bind the tRNA extra arm, because its cognate tRNA structures markedly deviate from the canonical cloverleaf secondary structure with highly truncated and/or intrinsically missing arms (40). Consequently, biochemical (41) and recent structural studies (19) have revealed a truly distinctive mode of tRNA binding by mammalian mitochondrial SerRS. The SerRSs from methanogenic archaea also differ markedly from their bacterial-type counterparts, most notably through the absence of the N-terminal coiled-coil (21). Besides its role in tRNA binding, the N-terminal domain of mMbSerRS is required to assist proper folding of the catalytic domain (25). Interestingly, archaeal SerRSs, either of archaeal/eukaryal- (17) or methanogenic-type, do not conserve the residues of *T. thermophilus* SerRS that interact with the tRNA extra arm (23, 26), although they can aminoacylate bacterial tRNAs^{Ser}, besides their homologous archaeal tRNA substrates (17, 29, 32). Therefore, it is possible that archaeal SerRSs recognize not only the

tRNA sequence, but also its overall three-dimensional structure that enables recognition of different tRNAs^{Ser} (32).

Identification of Amino Acids in the N-terminal Domain of mMbSerRS Critical for tRNA Recognition—We have demonstrated the contribution of individual amino acid residues toward tRNA binding, because their replacement leads to clear functional defects (see Table 1 and Figs. 2, 3, 5, and 7). The altered residues can have direct influence on tRNA binding (side chains that are in direct contact with tRNA) or indirectly affect interaction between the synthetase and tRNA (side chains that ensure proper positioning of amino acids involved in direct contact with tRNA). We demonstrate, by a range of methods, that the individual substitutions of Arg⁷⁶, Lys⁷⁹, and Arg⁹⁴ have a pronounced effect on the ability of the enzyme to serylolate cognate tRNA. The gel mobility shift assay showed that individual substitutions of these residues decrease the stability of SerRS•tRNA^{Ser} complexes (see Fig. 3). Binding analysis using SPR revealed that wild type archaeal mMbSerRS binds *in vitro* transcribed MbtRNA^{Ser} with high affinity (see Table 1). The determined dissociation constant ($K_D = 0.12 \mu\text{M}$) is similar to other synthetase•tRNA complexes (involving CysRS (42), GlnRS (43, 44), and AspRS (45)). The interaction between *M. barkeri* SerRS and tRNA is entirely lost after replacement of Arg⁷⁶, located in the short H2 helix, with alanine (see Figs. 1, 2, 3, and 6), preventing the estimation of the K_D . The most affected measurable tRNA binding affinity was for mutant R94A, the K_D value of which was increased about 50-fold relative to WT mMbSerRS. Arginine 94 is located in the loop between helix H2 and β -strand A4 and according to the docking model positioned to interact with the T-loop of the tRNA^{Ser}. The crystal structure of the SerRS•tRNA^{Ser} complex from *T. thermophilus* (23, 26, 46) revealed that the tRNA-binding coiled-coil of bacterial SerRS is buried between the T ψ C arm and the long extra arm of tRNA^{Ser}. Likewise, biochemical studies on the mammalian mitochondrial system pointed to the importance of the T-loop, which is the main identity element for two unusual tRNA^{Ser} isoacceptors. Previous kinetic analysis of variant tRNA^{Ser} transcripts by the mMbSerRS showed reduced serylation efficiency after abolishing interactions between the D- and T-loops, as these alterations, presumably, affected the tertiary structure of tRNA^{Ser} (27). The experiments presented here with the R94A mMbSerRS variant reveal the importance of the T-loop for interactions with methanogenic-type synthetase.

Alteration of Lys⁷⁹ (positioned in H2) strongly influences tRNA binding affinity, increasing the K_D 5-fold. Variants R94A and K79A aminoacylated tRNA^{Ser} with approximately one-third the velocity of the wild type enzyme, whereas the mutants carrying alanine at positions Arg³⁸, Lys¹⁴¹, Asn¹⁴², and Arg¹⁴³ remained moderately active, but also exhibited diminished affinity for tRNA, as expected. Arg³⁸, with a proline and two glycines in the vicinity (see Fig. 1A), is located in the loop between helix H1 and β -sheet A2 (see Fig. 1A). The flexibility of this region may be required for correct positioning of this mMbSerRS region toward tRNA. All other conserved amino acids in that area are hydrophobic and oriented to the interior of the enzyme, implicating their involvement in maintaining the structure of the N-terminal domain. Arg¹⁴³ has a dual role:

tRNA Binding Residues in mMbSerRS N-terminal Domain

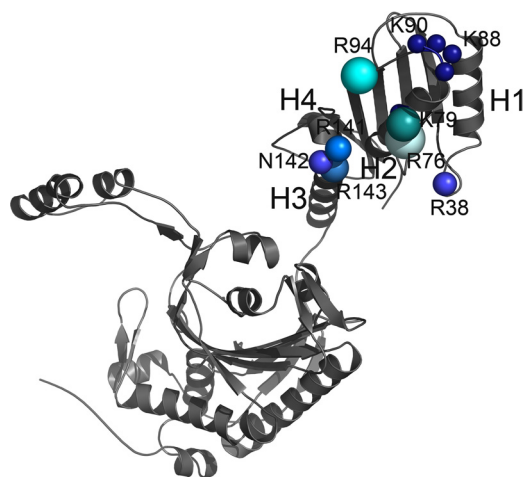


FIGURE 7. Contribution of the individual amino acids in tRNA binding. One subunit of the mMbSerRS dimer is shown. The size and the brightness of the spheres designate the significance of the particular residue in tRNA binding according to the cumulative influence on biochemical properties of mMbSerRS. The largest and the brightest sphere (arginine 76) annotates the most important side chain in tRNA recognition.

besides direct involvement in tRNA binding, its main chain also interacts with Arg¹⁴⁷, located in helix 4 that participates in helix-turn-helix-mediated positioning of the N-terminal domain relative to the catalytic core (25). Accordingly, the R143A variant binds cognate tRNA with 7-fold lower affinity (Fig. 7).

To assess whether selected N-terminal residues are important for aminoacylation *in vivo*, we tested the ability of corresponding mutant proteins to promote suppression of bacterial amber mutations. When the wild type mMbSerRS gene was introduced with MbtRNA^{Ser} to the *E. coli* strain bearing the *lacI-lacZ* fusion reporter system, robust β -galactosidase activity was produced (Fig. 6). In contrast, mutated SerRS genes promoted production of detectable, but less active reporter enzymes, in agreement with the K_D values estimated by SPR. Importantly, variant R76A was inactive in the suppression assay, even when coexpressed from the pBAD24 plasmid behind a stronger promoter. This confirms that the mutated enzyme(s) did not productively interact with tRNA^{Ser}, not only *in vitro*, but also in the cellular context, when competing noncognate tRNAs are present.

mMbSerRS Serylation Mechanism and the Importance of Substrate-induced Conformational Changes—Our previous crystallographic studies revealed that the binding of serine to wild type mMbSerRS causes a significant localized conformational change in the serine ordering loop (residues 394–410) of the enzyme (21). Next, positioning of the cognate tRNA in the active site of mMbSerRS is facilitated upon the conformational change of the motif 2 loop, which participates in ATP binding and mediates interactions with the tRNA acceptor stem (37). Our biochemical experiments point to the importance of the flexibility of the tRNA 3'-end binding region (37) for avoiding a steric clash as seen between the acceptor end of tRNA and the motif 2 loop Ile³⁴² in the tRNA·mMbSerRS complex model, and allowing hydrogen bonding of the first base pair.

The structure of the mMbSerRS enzyme shows that the orientation of N-terminal domains in two monomers differs by a

rotation of $\sim 20^\circ$ indicating that a conformational change likely accompanies tRNA binding (21). Accordingly, the SPR sensorgrams obtained for tRNA binding to immobilized WT mMbSerRS and the majority of constructed variants with mutations in the N-terminal domain agreed best with a two-state binding model implying that a conformational change occurs in the enzyme upon binding of the tRNA substrate (see Table 1 and Fig. 5). A two-step mechanism for the complex formation of synthetase and tRNA in the serine system from yeast was postulated in the mid-seventies (47, 48).

Our model suggests that the first step of binding will involve formation of a bimolecular complex between the tRNA and the flexibly disposed N-terminal domain of the SerRS. In the second step of the binding reaction, accommodation of the tRNA into the active site will occur, accompanied by conformational changes of the enzyme and the acceptor end of the tRNA. Nevertheless, our SPR binding experiments indicate that the second step of the binding is the rate-limiting step for the reaction and that this step is directly affected for all N-terminal domain mutants. These results suggest that the initial binding of the tRNA to the N-terminal domain is fast compared with the overall binding reaction. The slow step of the binding reaction involves the delivery of the tRNA to the active site of the enzyme, accompanied by the loss of entropy due to the organization of the flexibly disposed domains of the enzyme, and the associated conformational changes in the active site. During this second stage of the binding reaction the reduction in the affinity between the tRNA and the N-terminal domain, as indicated by the kinetic data obtained here, will increase the dissociation rate of the complex, perhaps by reducing the precision with which the tRNA is accommodated into the active site. Consequently, this would reduce the likelihood for the associated conformational changes in the active site of the enzyme that stabilize the interaction with the tRNA resulting in an increased k_{d2} of the binding reaction. A similar kinetic phenomenon was observed by Tsai and Johnson (49) of how T7 DNA polymerase discourages the incorporation of non-cognate nucleotides.

The different relative orientations of the tRNA-binding and catalytic domains were also shown to be associated with tRNA binding in yeast (50), *E. coli* AspRS (51), and human mitochondrial PheRS (52). Therefore, although tRNA-binding domains in the two SerRS types are non-homologous and evolutionarily unrelated (21), the requirement for a closing movement of the N-terminal domain upon tRNA binding has been observed in the *T. thermophilus* SerRS·tRNA co-crystal structure (23) and shown here for mMbSerRS.

Acknowledgments—We are grateful to Eilika Weber-Ban for useful suggestions regarding experimental procedures and for valuable discussions. Mike Scott and Stefan Schauer from the Functional Genomics Center, Zurich, are greatly acknowledged for assistance in SPR experiments. We are indebted to Rouven Bingel-Erlenmeyer and Martina Trokter for help with protein purification.

REFERENCES

1. Ibbra, M., and Soll, D. (2000) *Annu. Rev. Biochem.* **69**, 617–650
2. Eriani, G., Delarue, M., Poch, O., Gangloff, J., and Moras, D. (1990) *Nature*

- 347, 203–206
3. Cusack, S., Berthet-Colominas, C., Härtlein, M., Nassar, N., and Leberman, R. (1990) *Nature* **347**, 249–255
 4. Ibba, M., Morgan, S., Curnow, A. W., Pridmore, D. R., Vothknecht, U. C., Gardner, W., Lin, W., Woese, C. R., and Söll, D. (1997) *Science* **278**, 1119–1122
 5. Zhang, C. M., Perona, J. J., Ryu, K., Francklyn, C., and Hou, Y. M. (2006) *J. Mol. Biol.* **361**, 300–311
 6. Ataide, S. F., and Ibba, M. (2006) *ACS Chem. Biol.* **1**, 285–297
 7. Giegé, R., Puglisi, J. D., and Florentz, C. (1993) *Prog. Nucleic Acid Res. Mol. Biol.* **45**, 129–206
 8. Giegé, R., Sissler, M., and Florentz, C. (1998) *Nucleic Acids Res.* **26**, 5017–5035
 9. Nozawa, K., O'Donoghue, P., Gundllapalli, S., Arais, Y., Ishitani, R., Ume-hara, T., Söll, D., and Nureki, O. (2009) *Nature* **457**, 1163–1167
 10. Ribas de Pouplana, L., and Schimmel, P. (2001) *Cell* **104**, 191–193
 11. Ebel, J. P., Giegé, R., Bonnet, J., Kern, D., Befort, N., Bollack, C., Fasiolo, F., Gangloff, J., and Dirheimer, G. (1973) *Biochimie* **55**, 547–557
 12. Kim, H. S., Vothknecht, U. C., Hedderich, R., Celic, I., and Söll, D. (1998) *J. Bacteriol.* **180**, 6446–6449
 13. Tumbula, D., Vothknecht, U. C., Kim, H. S., Ibba, M., Min, B., Li, T., Pelaschier, J., Stathopoulos, C., Becker, H., and Söll, D. (1999) *Genetics* **152**, 1269–1276
 14. Lenhard, B., Orellana, O., Ibba, M., and Weygand-Durasevič, I. (1999) *Nucleic Acids Res.* **27**, 721–729
 15. Woese, C. R., Olsen, G. J., Ibba, M., and Söll, D. (2000) *Microbiol. Mol. Biol. Rev.* **64**, 202–236
 16. Fujinaga, M., Berthet-Colominas, C., Yaremchuk, A. D., Tukalo, M. A., and Cusack, S. (1993) *J. Mol. Biol.* **234**, 222–233
 17. Itoh, Y., Sekine, S., Kuroishi, C., Terada, T., Shirouzu, M., Kuramitsu, S., and Yokoyama, S. (2008) *RNA Biol.* **5**, 169–177
 18. Weygand-Durasevič, I., and Cusack, S. (2005) in *The Aminoacyl-tRNA Synthetases* (Ibba, M., Francklyn, C., and Cusack, S., eds) pp. 177–192, Landes Bioscience, Georgetown, TX
 19. Chimnarank, S., Gravers Jeppesen, M., Suzuki, T., Nyborg, J., and Watanabe, K. (2005) *EMBO J.* **24**, 3369–3379
 20. Sprinzl, M., and Vassilenko, K. S. (2005) *Nucleic Acids Res.* **33**, D139–D140
 21. Bilokapic, S., Maier, T., Ahel, D., Gruic-Sovulj, I., Söll, D., Weygand-Durasevič, I., and Ban, N. (2006) *EMBO J.* **25**, 2498–2509
 22. Thompson, J. D., Gibson, T. J., Plewniak, F., Jeanmougin, F., and Higgins, D. G. (1997) *Nucleic Acids Res.* **25**, 4876–4882
 23. Biou, V., Yaremchuk, A., Tukalo, M., and Cusack, S. (1994) *Science* **263**, 1404–1410
 24. Vincent, C., Borel, F., Willison, J. C., Leberman, R., and Härtlein, M. (1995) *Nucleic Acids Res.* **23**, 1113–1118
 25. Bilokapic, S., Ivic, N., Godinic-Mikulcic, V., Piantanida, I., Ban, N., and Weygand-Durasevič, I. (2009) *J. Biol. Chem.* **284**, 10706–10713
 26. Cusack, S., Yaremchuk, A., and Tukalo, M. (1996) *EMBO J.* **15**, 2834–2842
 27. Korencic, D., Polycarpo, C., Weygand-Durasevič, I., and Söll, D. (2004) *J. Biol. Chem.* **279**, 48780–48786
 28. Lesjak, S., and Weygand-Durasevič, I. (2009) *FEMS Microbiol. Lett.* **294**, 111–118
 29. Gruic-Sovulj, I., Jaric, J., Dulic, M., Cindric, M., and Weygand-Durasevič, I. (2006) *J. Mol. Biol.* **361**, 128–139
 30. Guzman, L. M., Belin, D., Carson, M. J., and Beckwith, J. (1995) *J. Bacteriol.* **177**, 4121–4130
 31. Coulondre, C., and Miller, J. H. (1977) *J. Mol. Biol.* **117**, 577–606
 32. Bilokapic, S., Korencic, D., Söll, D., and Weygand-Durasevič, I. (2004) *Eur. J. Biochem.* **271**, 694–702
 33. Yowler, B. C., and Schengrund, C. L. (2004) *Biochemistry* **43**, 9725–9731
 34. Chenal, A., Nizard, P., Forge, V., Pugnière, M., Roy, M. O., Mani, J. C., Guillain, F., and Gillet, D. (2002) *Protein Eng.* **15**, 383–391
 35. Normanly, J., Ogden, R. C., Horvath, S. J., and Abelson, J. (1986) *Nature* **321**, 213–219
 36. Polycarpo, C. R., Herring, S., Bérubé, A., Wood, J. L., Söll, D., and Ambrogely, A. (2006) *FEBS Lett.* **580**, 6695–6700
 37. Bilokapic, S., Rokov Plavec, J., Ban, N., and Weygand-Durasevič, I. (2008) *FEBS J.* **275**, 2831–2844
 38. Rogers, M. J., and Söll, D. (1988) *Proc. Natl. Acad. Sci. U.S.A.* **85**, 6627–6631
 39. Geslain, R., Aeby, E., Guitart, T., Jones, T. E., Castro de Moura, M., Charrière, F., Schneider, A., and Ribas de Pouplana, L. (2006) *J. Biol. Chem.* **281**, 38217–38225
 40. Helm, M., Brulé, H., Friede, D., Giegé, R., Pütz, D., and Florentz, C. (2000) *RNA* **6**, 1356–1379
 41. Shimada, N., Suzuki, T., and Watanabe, K. (2001) *J. Biol. Chem.* **276**, 46770–46778
 42. Zhang, C. M., Perona, J. J., and Hou, Y. M. (2003) *Biochemistry* **42**, 10931–10937
 43. Weygand-Durasevič, I., Schwob, E., and Söll, D. (1993) *Proc. Natl. Acad. Sci. U.S.A.* **90**, 2010–2014
 44. Bullock, T. L., Sherlin, L. D., and Perona, J. J. (2000) *Nat. Struct. Biol.* **7**, 497–504
 45. Frugier, M., Moulinier, L., and Giegé, R. (2000) *EMBO J.* **19**, 2371–2380
 46. Yaremchuk, A. D., Tukalo, M. A., Krikliiviy, I., Malchenko, N., Biou, V., Berthet-Colominas, C., and Cusack, S. (1992) *FEBS Lett.* **310**, 157–161
 47. Rigler, R., Pachmann, U., Hirsch, R., and Zachau, H. G. (1976) *Eur. J. Biochem.* **65**, 307–315
 48. Riesner, D., Pingoud, A., Boehme, D., Peters, F., and Maass, G. (1976) *Eur. J. Biochem.* **68**, 71–80
 49. Tsai, Y. C., and Johnson, K. A. (2006) *Biochemistry* **45**, 9675–9687
 50. Sauter, C., Lorber, B., Cavarelli, J., Moras, D., and Giegé, R. (2000) *J. Mol. Biol.* **299**, 1313–1324
 51. Rees, B., Webster, G., Delarue, M., Boeglin, M., and Moras, D. (2000) *J. Mol. Biol.* **299**, 1157–1164
 52. Klipcan, L., Levin, I., Kessler, N., Moor, N., Finarov, I., and Safro, M. (2008) *Structure* **16**, 1095–1104